Predicting torque of wool worsted single yarns using an efficient radial basis function network-based method

[1]Canh-Dung Tran and [2]David Graham Phillips

[1,2] Textile and Fiber Technology, CSIRO,

P.O. Box 21, Belmont, Victoria, 3216, Australia.

Abstract

The torque in single-spun yarns is an inherent property of the twisting and bending of staple fibres during the formation of yarn combined with the effect of applied tension on the yarn. The consequences of yarn torque are well known and are widely observed as yarn instability, e.g., yarn rotation under tension; local snarling and entanglement at low loads, and as distortion in fabric, i.e., edge-curl and skewing in knitted fabric. In this paper, a method for predicting the yarn torque based on the radial basis function networks is presented and evaluated. This method uses a "universal approximator" based on neural network methodology to minimize noise during training of the network and to approximate the yarn torque as a function of the geometrical and physical parameters of yarns (twist, linear density) and the applied load. The current method is an integral radial basis function network-based approach suitable for textile engineering and gives very good prediction of yarn torque across a range of yarn structural parameters and test conditions.

Key words:

Radial basis function networks, feed forward neural networks, yarn structural parameters, yarn instability, intrinsic torque

1. Introduction

For several decades now, various neural network (NN) models have been applied to many problems in different disciplines such as physics, engineering, and computer science. Among the NN-models, the multi-layer perceptron networks (MLPNs) and radial basis function networks (RBFNs) have emerged as the leading classes. These feed forward neural networks (FFNN) have the advantage that

the approximations used allow the network to learn and predict non-linearity in the input and output parameters. This feature makes these systems very suitable for dealing with the

behaviour of non-linear relationships that are common in textile engineering. Neural network models have been applied to many different areas of cotton processing and performance: yarn hairiness (Babay *et al*., 2004), spinning performance (Beltran *et al*., 2004; Pynckels *et al*., 1997), yarn strength (Cheng and Adams, 1995), yarn ten-sile properties (Ramesh *et al*., 1995) and fabric properties (Fan and Hunter, 1998), and the relationships between fibre properties and the strength of open-end spun yarns (Ethridge *et al*., 1982). Furthermore, Basu *et al*. (2002) employed an artificial NN to study the relationship between yarn and fabric handling properties. While most of the research studies published so far have been based on MLPNs, Behera and Muttagi (2004) employed RBFNs to predict the properties of woven suiting fabrics. In this paper, an integral RBFN-based approach is evaluated against a conventional RBFN method and is applied to the prediction of the torque of wool worsted single yarns with respect to the yarn parameters. In the second section the background to the modelling and measurement of yarn torque is described. In the third section, an introduction to Multi-Quadric Radial Basis Function Networks (MQRBFNs) is provided. The fourth section details the algorithms used to train the MQ-RBFNs in predicting yarn torque, particularly the use of a model that reduces noise during the training of the NN. In the fifth section the performance of integral RBFN methods is compared with a conventional RBFN method using torque data for training these systems. An evaluation of the accuracy of the preferred integral RBFN model is made with several different training sets from the torque data set and this shows excellent predictability across a wide range of experimental conditions.

2. YARN TORQUE

Yarn torque is formed in a freshly spun worsted yarn and is well known as twist-liveliness causing snarling and entanglement of yarn at low tensions. Platt *et al*. (1958) derived the torque in a spun yarn from the torsional and bending moments of the fibres using an idealised helical geometry for the fibres in the yarn and without applied tension. The key geometrical variables influencing the yarn torque were number of fibres (yarn count) and yarn radius (yarn count) $^{1/2}$, as well as a complex function of the surface helix angle (twist) and the fibre elastic moduli.

Postle *et al*. (1964) showed the importance of applied tension in generating yarn torque. The torque due to tension was remodeled by Bennett and Postle (1979) to allow for the effect of fibre migration and showed that the torque due to tension dominates the total yarn torque

under even moderate tensions; see also Tandon *et al*. (1995) and Grishanov *et al*. (1997). The Postle models identified the importance of yarn radius (yarn count)$^{1/2}$, the surface helix angle (twist), and the applied load. Dhingra and Postle (1974a, 1974b) used Postle's model of yarn torque due to tension to calculate the presence of a net torque at zero applied tension. More recently, Mitchell *et al.* (2006) developed a direct measurement technique to obtain the two components of torque in a ring-spun worsted yarn, i.e., (i) the torque due to the applied tension, and (ii) the intrinsic torque that exists in the yarn at zero applied tension due to bending and twisting of fibres during yarn formation.

These experiments by Mitchell *et al*. (2006), on a limited range of samples, showed relationships that were consistent with the parameters identified in the models of yarn torque above, such as twist and yarn count, the effect of yarn steaming and the test environment, i.e., in both dry and wet conditions. A complex variation in the results was apparent depending on the yarn geometry and history across a small set of samples. The modelling of yarn torque is a key step in identifying the contribution of torque to yarn instability and fabric distortions, e.g., yarn snarling and fabric spirality or skewing. In practice, steaming and setting of yarn can provide temporary and partial relief to the problem or two-plying of singles can be used to obtain a low torque yarn. Fabric skewing is recognized as having a link to yarn torque but the individual contributions of the torque due to tension and the intrinsic torque have not been resolved.

Incipient snarling can occur as tensioned yarn is twisted above a critical value or as the tension in a twisted yarn is reduced. Application of complexity theory to rods shows that the formation of an incipient snarl is the manifestation of a non-linear system with a transition jump from one state to another (Van der Heijden and Thompson, 2000). Other workers have linked snarling to yarn twist, yarn tension, yarn bending, and yarn torsional stiffness, factors that are closely related to yarn torque. Consequently, in order to address some of these complex problems and applications of yarn instability, an accurate estimate is needed of the torque levels operating across typical parameters used in industry.

The torque measurement technique used at CSIRO by Mitchell *et al*. (2006), allows the total torque in a single strand of yarn to be measured directly using a hank while under tension. In this work an RBFN-based non-linear modelling approach is employed to predict the torque of wool worsted single yarns using the data obtained from this experimental technique applied to a wide range of worsted yarn types. The key yarn parameters explored are those identified

theoretically and experimentally, as outlined above, including yarn linear density, yarn twist and applied tension.

3. MULTI-QUADRIC RADIAL BASIS FUNCTION NETWORKS

Radial basis function networks are widely and successfully used to predict the properties of complex data sets. The linear combination of nonlinear radial basis functions is the key to the RBFN's ability to model the data while allowing computational and analytical ease of use.

In principle, it is possible to approximate any smooth function $y(\mathbf{x})$ with RBFNs (Haykin, 1999). The present work uses linear RBFNs with one hidden layer of radial basis functions where the approximation function $f(\mathbf{x})$ of $y(\mathbf{x})$ is decomposed into m fixed RBFs as follows (Figure 1 shows a schema of a fully connected RBFN):

$$y(\mathbf{x}) \approx f(\mathbf{x}) = \sum_{j=1}^{m} w^j h^j(\mathbf{x}) \qquad (1)$$

where $\{w^j, j = 1..m\}$ is the set of network weights, h^j the chosen radial basis function corresponding to the j^{th} neuron, m the number of RBFs. Let n is the number of data points $\left\{\mathbf{x}^p, y^p\right\}_{p=1}^{n}$ where $\mathbf{x}^p$ is the coordinate of the p^{th} collocation point and y^p is the desired value of function y at the point $\mathbf{x}^p$, usually $m \le n$ (Haykin, 1999). Each of d components of $\mathbf{x}$ feeds forward to *m* basis function neurons whose outputs are linearly combined weights into the network output $f(\mathbf{x})$.

The MQ-RBF is recognized mathematically (Franke, 1982) for giving better approximation results compared with the other RBFs, e.g., Gaussian. Hence, a global MQRBF is employed in this work and given by

$$h^j(r) = h^j\left(\left\|\mathbf{x} - \mathbf{c}^j\right\|\right) = \sqrt{\mathbf{r}^2 - \mathbf{a}^{(j)2}} \qquad (2)$$

where $\mathbf{r} = (\mathbf{x} - \mathbf{c}^j)$ and $r = \left\|\mathbf{x} - \mathbf{c}^j\right\|$ is the Euclidean norm of $\mathbf{r}$; $\mathbf{c}^j$ is a set of centers that can be chosen from among the data points; $a^j > 0$ is the width of the j^{th} RBF (Haykin, 1999). The accuracy of the MQ-RBF approximation is dependent on the width of the RBF (Kansa, 1990; Park and Sandberg, 1991; Carlson and Foley, 1991), whose choice is still an open question. In the present work, the set of centers is the same as the set of training points and the width a^j is computed as follows

$$a^j = \alpha d^j \tag{3}$$

where α is a chosen coefficient and d^j is the minimum of distances from the j^{th} center to neighbors. Since the function f(**x**) is expressed as a weighted linear combination of RBFs, it can be differentiated or integrated. Hence, the differential or integral functions are the weighted linear combinations of basics functions.

4. MODELLING TORQUE USING THE MQ-RADIAL BASIS FUNCTION NETWORK-BASED APPROACHES

In this section, two MQ-RBFN-based modelling approaches, the conventional MQ-RBFNs and the modified MQ-RBFNs, are defined for use in approximating a complex function. These two sections explain the development of these approaches for reducing the noise or error in the models in detail to allow the further use of this approach by other researchers.

4.1 Conventional RBFN approach (C_RBFN)

The conventional method was presented and employed firstly by Hardy (1971) in approximating surfaces. It then has been efficiently applied to many different areas (Kansa, 1990; Zerroukat et al, 2000 and Tran-Canh and Tran-Cong, 2002a). The approach uses RBFNs to model an original function y based on the set of training data $\left\{\mathbf{x}^p, y^p\right\}_{p=1}^n$ obtained from experimental measurements. With the model $f(\mathbf{x})$ constructed as a linear combination of m MQ-RBFs (Equation (1)), the problem is to determine the unknown weights $\{w^j\}$, $j = 1,\ldots,m$ of the network. The training of the model can be achieved via minimization of a cost function based on the sum of squared errors. To counter the effects of over fitting or noise, a roughness penalty term can be added to the cost function (Haykin, 1999; Tran-Canh and Tran-Cong, 2002a) to produce

$$C(\mathbf{w},\lambda) = \sum_{p=1}^{n}\left(y^p - f\left(\mathbf{x}^p\right)\right)^2 + \lambda\sum_{j=1}^{m}\left(w^j\right)^2 \tag{4}$$

where λ is the global regularization parameter. Given a choice for λ, the minimization of the cost function (4) yields an optimal weight vector $w = \left(w^1, w^2, \ldots, w^m\right)^T$ according to

$$\mathbf{Q}\mathbf{w} = \mathbf{H}^T\mathbf{y} \tag{5}$$

where **H** is the design matrix with $H_{ij} = h^j\left(\mathbf{x}^i\right), (i = 1..n, j = 1..m)$ and $\mathbf{y} = \left(y^1, y^2, ..., y^n\right)^T$ is the n-dimensional vector of training output values. $\mathbf{Q} = \mathbf{H}^T\mathbf{H} + \lambda\mathbf{I}$ is the variance matrix and **I** is the identity matrix. There are several heuristics for the estimate of λ (Sen and Srivastava, 1997; Haykin, 1999) of which the generalized cross-validation is used in the present work to optimize the regularization parameter λ. In the case λ = 0 (non regularization) and m = n, Eq. (5) is rewritten as follows

$$\mathbf{Hw} = \mathbf{y} \tag{6}$$

Therefore, there is only one "training pattern" and the network weights are found in a single general linear least square procedure. In order to avoid the presence of round-off errors because of the high condition number of the normal matrix, the method of orthogonal triangle decomposition with pivoting (Bjorck, 1996) is employed to solve this least-squares problem

4.2 Modified multi-quadric radial basis function network approach (M-RBFN)

The modified approach was developed by Mai-Duy and Tran-Cong (2001) to solve rheological problems in fluid dynamics, in which the integration of first or second order derivatives was used to reduce the sensitivity of noise. In the modified approach, the initial highest order derivatives that are identified for function $f(\mathbf{x})$ are expressed by RBFNs, which are integrated to determine the lower order derivatives and the function $f(\mathbf{x})$. This is explained in the following using a function of two variables with two cases. In (a) the first order derivatives of a function $f(\mathbf{x})$ are expressed by RBFNs and in (b), the second order derivatives are expressed by RBFNs.

Modeling a function from their first order derivative functions (M1-RBFN)

In this approach, named M1-RBFN, the first order partial derivative of f(**x**) with respect to x_i (i = 1,2) is approximated as follows

$$\frac{\partial f\left(\mathbf{x}\right)}{\partial x_i} = \sum_{j=1}^{m} w^j h^j\left(\mathbf{x}\right) \quad (i = 1,2) \tag{7}$$

The original function can be determined by

$$y(\mathbf{x}) \approx f(\mathbf{x}) = \int \frac{\partial f(\mathbf{x})}{\partial x_i} dx_i = \int \left(\sum_{j=1}^{m} w^j h^j(\mathbf{x}) \right) dx_i = \sum_{j=1}^{m} w^j \int h^j(\mathbf{x}) dx_i$$
$$= \sum_{j=1}^{m} w^j g^j(\mathbf{x}) + C_o(x_k), k = 1,2; k \neq i \quad (8)$$

where $g^j(\mathbf{x}_i)\big|_{j=1}^{m}$ is the set of basis functions corresponding to RBFs (h^j) and is determined by integrating the MQ-RBF as follows

$$g^j(\mathbf{x}) = \frac{(x_k - c_k^j)\sqrt{r^2 + a^{(j)2}}}{2} + \frac{r^2 - (x_k - c_k^j)^2 + a^{(j)2}}{2} \left(Ln(x_k - c_k^j) + \sqrt{r^2 + a^{(j)2}} \right) \quad (9)$$

and $C_o(x_k)$ (the integration constant) is a function of the variable $x_k (k \neq i)$ and also approximated using the M2-RBFN-based method (see next section) but for one dimensional functions of x_k as follows:

$$\frac{d^2 C_o(x_k)}{dx_k^2} = \sum_{j=m+1}^{m+t} w^j h^j(x_k), k \neq i$$
$$\frac{dC_o(x_k)}{dx_k} = \sum_{j=m+1}^{m+t} w^j g^j(x_k) + C_o^1 \quad (10\ a,b,c)$$
$$C_o(x_k) = \sum_{j=m+1}^{m+t} w^j l^j(x_k) + C_o^1 x_k + C_o^2$$

where C_o^1, C_o^2 are integral constants, t is the number of centers (corresponding to weights $w^j\big|_{j=m+1}^{m+t}$ w^j) whose x_k coordinates are distinct. The unknown of the problem consists of a set of weights $\{w^j\}_{j=1}^{m+t}$ and C_o^1, C_o^2 of a system of linear equations which is obtained by applying the principle of linear least square as presented in the fourth section using Equations (8), (9), 10(b), and 10(c).

Modeling a function from a second order derivative functions (M2-RBFN)

For this modeling approach, the RBFNs are used to represent the second derivatives ($\partial^2 f / \partial x_i^2, (i = 1,2)$), the first order derivatives $\partial f / \partial x_i$ and the function can be then determined as follows

$$\frac{\partial^2 f(\mathbf{x})}{\partial x_i^2} = \sum_{j=1}^{m} w^j h^j(\mathbf{x}) \tag{11}$$

$$\frac{\partial f(\mathbf{x})}{\partial x_i} = \int \left(\sum_{j=1}^{m} w^j h^j(\mathbf{x}) \right) dx_j = \sum_{j=1}^{m} w^j g^j(\mathbf{x}) + C_o(x_k) = \sum_{j=1}^{m+t_1} w^j g^j(\mathbf{x}) \tag{12}$$

$$f(\mathbf{x}) = \int \left(\sum_{k=1}^{m+t_1} w^j g^j(\mathbf{x}) + C_o(x_k) \right) dx_k = \sum_{j=1}^{m} w^j l^j(\mathbf{x}) + C_0(x_k) x_k + C_1(x_k) = \sum_{j=1}^{m+t_2} w^j l^j(\mathbf{x}) \tag{13}$$

where $l^j(x)$ is given by integrating equation (9)

$$\begin{aligned} l^j(\mathbf{x}) &= \int g^j(\mathbf{x}) dx_k \\ &= \frac{\left(r^2 + a^{j2}\right)^2}{6} + \frac{r^2 - \left(x_k - c_k^j\right)^2 + a^{(j)2}}{2} \left(x_k - c_k^j\right) Ln\left(\left(x_k - c_k^j\right) + \sqrt{r^2 + a^{(j)2}} \right) \\ &\quad - \frac{r^2 - \left(x_k - c_k^j\right)^2 + a^{(j)2}}{2} \sqrt{r^2 + a^{(j)2}} \end{aligned} \tag{14}$$

where $C_o(x_k), C_1(x_k)$ are integration constants and calculated using the same way mentioned in section 4.2.a; t_1 and t_2 ($t_2 = 2t_1$) are the number of centers to represent these integration constants. They are the number of additional weights from the approximation of integration constant C_o and C_1. In this work, the new centers in the approximation of integration constants are chosen to be distinct x_k coordinates of data points. The strategy of training to obtain the model of the original function f(**x**) is described in the fourth section.

Identical conditions

For approximation of a function of two or more variables using the M2-RBFN method, since there are different starting points which can be used to determine partial derivatives, it is necessary to impose some constraints on functional networks to obtain the original function. Let $(.)_{x_k}$ be the results obtained by the integration of (.) with respect to x_k, an algorithm of the method can be rewritten as follows:

$$\frac{\partial^2 f}{\partial x_1^2} \to \frac{\partial f}{\partial x_1} \to f_{x_1}(\mathbf{x}), \quad \frac{\partial^2 f}{\partial x_2^2} \to \frac{\partial f}{\partial x_2} \to f_{x_2}(\mathbf{x}), \tag{15}$$

where $f_{x_1}(\mathbf{x})$ and $f_{x_2}(\mathbf{x})$ are two approximating representations for the function f(**x**) corresponding to the two starting points $\frac{\partial^2 f}{\partial x_1^2}$ and $\frac{\partial^2 f}{\partial x_2^2}$, respectively. Hence, the identical condition needs to be imposed as follows

$$f_{x_1}(\mathbf{x}) = f_{x_2}(\mathbf{x}) = f(\mathbf{x}) \tag{16}$$

With a given set of training data $\{\mathbf{x}^i\}_{i=1}^n$ the identical conditions yield to a system of equations as follows:

$$\frac{\partial^2 f(\mathbf{x})}{\partial^2 x_1} = \mathbf{H}(\mathbf{x})\mathbf{w}_{x_1} \rightarrow \frac{\partial f(\mathbf{x})}{\partial x_1} = \mathbf{G}_{x_1}(\mathbf{x})\mathbf{w}_{x_1} \rightarrow f_{x_1}(\mathbf{x}) = \mathbf{L}_{x_1}(\mathbf{x})\mathbf{w}_{x_1} \tag{17}$$

$$\frac{\partial^2 f}{\partial^2 x_2} = \mathbf{H}(\mathbf{x})\mathbf{w}_{x_2} \rightarrow \frac{\partial f}{\partial x_2} = \mathbf{G}_{x_2}(\mathbf{x})\mathbf{w}_{x_2} \rightarrow f_{x_2}(\mathbf{x}) = \mathbf{L}_{x_2}(\mathbf{x})\mathbf{w}_{x_2} \tag{18}$$

$$\mathbf{L}_{x_1}(\mathbf{x})\mathbf{w}_{x_1} = \mathbf{L}_{x_2}(\mathbf{x})\mathbf{w}_{x_2} \tag{19}$$

where w_{x_i} is the sets of the network weights to be found and **H**, **G**, **L** the design matrices corresponding to the second derivative, first derivative, and the function, respectively; Hence, the unknown vector in the modified approach is $(w_{x_1}; w_{x_2}; ...; w_{x_d})$ in which the length of each $\mathbf{w}_{x_i}$ is $(m + t_2)$ and d is the dimensionality of the input vector.

4.3 The approach used for modelling yarn torque

The RBFN based methods are applied here to model torque of wool worsted single yarns. In this work, torque (**y**) is considered as the function of a vector variable (**x**) consisting of yarn count (x_1), twist (x_2), and applied tension (x_3) and acting as inputs of RBFNs. The analysis employs yarn torque data obtained at CSIRO. The relationship between yarn torque and applied tension of yarns is considered on a wide range of yarn linear densities (22.8–80 tex), metric twist factors (50–140), and applied tension (0.005–0.1052 N). For building the models, the data were divided into two groups, i.e., training data and test data, and the evaluation of models was carried out by using a *L*2 norm of the error (*N*e), which is defined as follows:

$$N_e = \sqrt{\sum_{i=1}^{t}\left(y^i - f(\mathbf{x}^i)\right)^2} \tag{20}$$

where y_i and $f(x_i)$ are the measurement values and prediction values using the RBFN methods at the vector variables $\mathbf{x}^i = \left(x_1^i, x_2^i, \cdots, x_n^i\right)$ and t is the number of test data. The value of N_e decreases as the accuracy of the prediction increases. In order to reduce the floating error during training, the training data were normalized so that they were bounded within the prescribed range of 0 and 1. Scaling was carried out by dividing each value by the maximum value of the overall data, and the predicted values of networks were post-processed by multiplying them by the maximum value of the overall training data. In this paper, the prediction of torque is modelled for conventional ring spun yarns, when tested in both wet and dry conditions.

5. EVALUATION OF THE RADIAL BASIS FUNCTION NETWORK-BASED MODELS, RESULTS, AND DISCUSSION

5.1 Comparison of the performance of the radial basis function networks-based models

It is well documented that the training of RBFNs is much faster than the other FFNNs such as MLPNs (Behera and Muttagi, 2004; Haykin, 1999; Tran-Canh and Tran-Cong, 2002b), and in the present work, the performance of the modified RBFN-based model outlined above was evaluated by comparing the errors of the prediction with other methods.

A set of 210 data were employed with 180 input–output pairs used for training the networks and 30 pairs of data were retained for testing the trained network. Neural networks were trained to predict the torque of un-steamed and steamed wool worsted single yarns in dry conditions (standard condition of laboratory) and in wet conditions. The centres of networks were taken to be the set of training data in the present work, i.e., $\mathbf{x}^i = \mathbf{c}^i$, (i = 1, . . . , n). The width of the j^{th} RBF was determined as presented in Equation (3). The performance of models was evaluated by error norms calculated by Equation (20). Table 1 shows typical error norms (N_e) of yarn torque for two conditions of testing with the three different RBFN methods using the coefficient α = 3.0. It can be seen that prediction performance of the M2-RBFN method is always better than others for un-steamed yarns in both dry and wet conditions, that is, the error of the prediction is least.

For the MQ-RBFN-based methods, the coefficient α influences the accuracy of the prediction. The effect of the value of α on the models is shown in Figures 2 and 3. In all cases the M2-RBFN method shows the least error.

5.2 Predicting total torque in yarn under tension

The previous section confirmed the superiority of the M2- RBFN approach. In this section theM2-RBFN method is assessed by application to the prediction of the yarn torque. The structural parameters of the experimental set of wool worsted yarns included yarn linear density, twist, and applied tension. The related torque measurements were made across a range of tensions per yarn strand from 0.44 to 11.9 cN using both wet and dry conditions on yarns that were steamed after spinning and unsteamed. The yarn torque training data and the test data were selected from the experimental database. In all these measurements the yarn torque data act as output targets to the networks for training and testing purpose. Before feeding to the network, each input–output data set was scaled down to be within the range (0, 1) as presented in the previous section.

Analysis of steamed yarns

The test data was based on 21.8 μm wool worsted single yarns, steamed at 87^{o}C (two cycles of 5 min). The yarn linear density ranged from 22.9 to 63.6 tex (seven steps of yarn count) and at each yarn count the yarns were spun at 60 to 140 metric twist factor (at intervals of 20, i.e., five steps) forming a range of yarn twist from 239 to 925 tpm.

The torque behaviour of yarns was predicted in both dry (normal laboratory conditions) and wet test conditions. The M2-RBFN-based model was investigated with three sets of testing data corresponding to different yarn counts 28 tex, 48.3 tex, and 56 tex, e.g., in the first case the model was established using the data set without the 28 tex data and the model then applied to predict the 28 tex set of data. This approach was taken to further test the use of theM2-RBFN to the data set, which was limited in size.

Figure 4 indicates the total torque of wool worsted yarns whose count is 28 tex with respect to tension and twist in the dry and wet conditions. Similarly, Figure 5 depicts torque of 48.3 tex wool worsted yarns and Figure 6 shows the torque of 56 tex yarns in the dry and wet conditions. In each case the correlation coefficient ($\boldsymbol{R^2}$) was calculated for the predicted results and experimental results and for the six trials the correlation coefficient was better than 0.983 (see legends to the figures). This evaluation again shows the ability of the M2-RBFN to accurately model the data, and the shapes of the surfaces shown in the figures highlight the non-linear relationships between yarn torque, tension, the yarn twist, and yarn count.

Figure 7 shows the plot of the predicted yarn torque versus the experimental yarn torque measured at CSIRO for the set of data corresponding to Figure 4 (left-side diagram). The

standard error between values predicted by the M2-RBFN method and from the experimental results was 0.031 with R^2 = 0.991. A similar analysis using C-RBFN showed a R^2 = 0.96.

Un-steamed yarns

A separate data set of 108 results was used for the unsteamed case using 21.8 μm wool worsted yarns spun to 30, 50, and 80 tex with a range of metric twist factors at each yarn count, usually 50 to 140 and with six tensions. Since ageing is an important factor affecting the yarn torque of un-steamed yarns when measured in dry conditions, the M2-RBFN evaluation used yarn torque data measured at around 30 days after spinning. The torque prediction was evaluated for two separate groups of testing data, the metric twist factors and applied tensions. Again the RBFN model was prepared on a training set of data, typically 90 results, and the predictions were tested against the remainder of the experimental test data. Figures 8 and 9 show the torque values predicted using this approach for wool worsted yarns with twist factors of 80 and 120, plotted against tension and yarn count in both dry and wet conditions.

Figures 10 and 11 describe the torque of wool worsted yarns imposed by applied tensions 4.89 cN and 7.1 cN in the dry conditions and 4.31 cN and 6.28 cN in the wet conditions respectively plotted against twist and yarn count. For the case of unsteamed yarns, although the training set is smaller and the data are fewer than in the previous steamed case, the coefficient of correlation between the predicted results and the measured results are around 0.96 and the maximum relative errors were less than 8%.

The high correlation coefficients shown for all of the comparisons between the experimental measurement and predicted torque values of wool worsted yarns based on the structural parameters of the yarns demonstrate the ability of the M2-RBFNs to efficiently simulate the nonlinear structural property relationships of the wool worsted yarns. The RBFN approach allows any nonlinear response of yarn torque to the tension, twist and linear density in this range of yarns evaluated to be predicted and applied to the study of instability in worsted yarns.

5.3 Predicting intrinsic torque using M2-radial basis function networks

The intrinsic torque, the torque at zero tension, was also predicted using the present method. Since this is an extrapolation of the model to zero tension, a series $\{P^j\}_j^k$ =1 of predicting steps was carried out with a descending range of k (k =10) different values of tension from the

minimum load tension used in experimental measurement [0.005 N] to zero load [0.00400, 0.00250, 0.00150, 0.00100, 0.00060, 0.00040, 0.00035, 0.00010, 0.00005, 0]. The training algorithm used added the predicted torque at the step j to the set of training data of the next predicting step (j+1), i.e., if $\{(x_i , y_i)i = 1,...,n \}\ j$ is the set of training data corresponding to Pj then the training data set of the next step Pj+1 will be $\{(x_i , y_i)\ i = 1,...,n+1\}\ j$+1 in which yn+1 was predicted from the previous step. The results show that the predicted intrinsic torque values are about 10% higher than the values obtained from the intersection of a linear line of best fit between torque and tension as used at CSIRO to estimate the intrinsic torque (see Table 2). This difference, while small, may be due to non-linearity of the model and the process of extrapolation from the original set of data.

CONCLUDING REMARKS

This paper reports the employment of a second order multi-quadric RBFN based approach to predict the yarn torque behaviour of wool worsted single yarns as a nonlinear function of their structural parameters (twist, linear density, and applied load). The analysis showed that although other MQ-RBFN-based approaches (conventional and first order RBFNs) offer good performance in accuracy based on error norms, the M2-RBFN-based approach achieves the greatest accuracy. In other words, with the same accuracy, the modified approach requires a smaller set of training data. In spite of the limited size of the data base used in this study, the training process using the real data from CSIRO demonstrated that the second order RBFN approach provides a suitable tool for predicting wool worsted yarn properties and allows the yarn torque to be estimated with confidence across a wide range of yarn parameters.

Acknowledgements

The authors thank J. Marsh, J. Hair, and L. Staynes (CSIRO, Textile and Fibre Technology) for measuring and compiling the yarn torque data. The yarn torque data was obtained through a project funded by Australian Wool Innovation, Australia on behalf of the Australian woolgrower and the use of the data is much appreciated. This work was also supported by a grant of computing time from Australia Partnership for Advanced Computing (APAC) National Facility. Canh-Dung Tran is supported by a CSIRO Postdoctoral Research Fellowship. All of this support is gratefully acknowledged.

References

Babay, A., Cheikhrouhou, M., Vermeulen, B., Rabenasolo, B. and Castelain, J.M., 2004, Selecting the optimal neural network architecture for predicting cotton yarn hairiness, The textile Institute, 96(3), 185-192.

Basu, A., Chellamani, K.P. and Ramesh Kumar P., 2002, Fabric engineering by means of an Artificial Neural Network, J. Text. Inst., 93(3), 283-296.

Behera B.K. and Muttigi, S.B., 2004, Performance of error back propagation vis a vis Radial Basis Function Neural Network. Part I: Prediction of Properties for Design Engineering of Woven Suiting Fabrics, J. Textile Inst, 95, 284-300.

Beltran, R., Wang, L. and Wang, X. 2004, Predicting worsted spinning performance with Artificial Neural Network model, Textile Res. J. 74(9), 757-763.

Bennett, J. M. and Postle, R., 1979, A study of torsional stability in plied yarns, J. Text. Inst., 4, 142 – 151.

Bjorck, A., 1996, Numerical methods for least squares problems, Philadelphia, SIAM.

Carlson, R.E. and Foley, T.A., 1991, The parameter R^2 in multiquadric interpolation, Computers Math. Applic. 21(9), 29-42.

Cheng, L. and Adams, D., 1995, Yarn strength prediction using Neural Networks, Part I: Fiber properties and yarn strength relationship, Textile Res. J. 65(9), 495-500.

Cybenko, G., 1989, Approximation by superposition of sigmoidal function. Mathematics of control signals and systems, 2, 303-314.

Ethridge, M.D., Tower, J.D., and Hembree, J.F., 1982, Estimating functional relationships between fiber properties and the strength of open-end spun yarns, Textile Res. J. 52, 35-45.

Fan, J. and Hunter, L., 1998, A worsted Fabric Expert System, Part II: An Artificial Neural Network model for predicting the properties of Worsted Fabrics, Textile Res. J 68(10), 763-771.

Franke, R., 1982, Scattered data interpolation: test of some methods, Math. Comput. 48, 181-200.

Grishanov, S.A., Lomov, S.V., Cassidy, T. and Harwood, R.J., 1997, Simulation of Geommetry of a two-component yarn Part II: Fiber distribution in the yarn cross-section, J. Text. Inst., 88(4) Part 1.

Hardy, R.L., 1971, Multiquadric equations for topography and other irregular surfaces, J. Geophys. Res. 176, 1095-1915.

Haykin, S., 1999. Neural networks: A comprehensive foundation. New Jersey: Prentice Hall.

Hornik, K., Stinchcombe, M. and White, H., 1989. Multilayer feed-forward networks are universal approximators. Neural networks, 2, 359-366.

Jasper, W.J., and Kovacs, E.T., 1994, Using Neural Networks and NIR Spectrophotometry to Identify Fibers, Textile Res. J. 64(8), 444-448.

Kansa, E.J., 1990, Multiquadrics - A scattered data approximation scheme with applications to computational fluid dynamics-I: Surface approximations and partial derivatives estimates. Comput. Math. Appl., 19(8-9), 127-145.

Lamb, R.P., and Yang, S., 1996, Choosing the right top for spinning, Top-tech Int, Wool secretariat, CSIRO Australia, 258-276.

Liberman, M.A., and Patil, R.B., 1994, Clustering and Neural Networks to Categorize Cotton Trash, Opt. Eng. 33(5), 1642-1653.

Mai-Duy, N. and Tran-Cong, T., 2001, Numerical solution of Navier-Stokes equations using multiquadric radial basis function networks, Neural Networks 14, 185-199.

Park, J. and Sandberg, I.W. 1991. Universal approximation using radial basis function networks. Neural Computation, 3, 246-257.

Phillips, D.G., 2005, Yarn instability FT405: Part 3, Data set and analysis on untreated and SR wool yarns, twist-liveliness, spirality and plied yarn results, Report, TFT, CSIRO.

Poggio, T. and Girosi, F., 1990. Networks for approximation and learning. In: Lau, C. (Ed), Neural Networks: Theoretical foundations and analysis, 91-106, New-York: IEEC Press.

Pynckels, F., Kiekens, P., Sette, S., Van Langenhove, P. and Impe, K., 1997, Use Neural Nets to simulate the spinning process. J. Textile Inst. 88(4), 440-447.

Ramesh, M.C., Rajamanickam, R., and Jayaraman, S., 1995, Prediction of yarn tensile properties by using Artificial Neural Network, J. Text. Inst., 86, 459-469.

Sen, A. and Srivastava, M., 1997, Regression analysis: theory, methods and applications. Berlin: Springer.

Tandon, S. K., Carnaby, G. A., Kim, S. J. and Choi, F. K. F., 1995, The Torsional behavior of singles yarns, Part I: Theory, J. Text. Inst., 86(2), 185 – 199.

Tran-Canh, D. and Tran-Cong, T., 2002a, BEM-NN computation of Generalised Newtonian Flows, J. Eng. Anal. with Boundary Elements. 26, 15-28.

Tran-Canh, D. and Tran-Cong, T., 2002b, Computation of viscoelastic flow using Neural Networks and Stochastic Simulation. KARJ, 14(4), 161-174.

J. M. T., 2000.

Helical and localised buckling in twisted rods: A unified analysis of the symmetric case, Nonlinear Dynam., 21, 71–99.

Table 1 Comparison of error norms (N_e) of the torque prediction between the C-RBFN, M1-RBFN, and M2-RBFN methods at the applied tension = 0.043 N for steamed yarns and 0.048 N for unsteamed yarns

	Unsteamed yarns		Steamed yarns	
	Dry	Wet	Dry	Wet
C-RBFN	3.05e–001	3.06e–001	2.07e–001	3.12e–001
M1-RBFN	1.71e–001	1.425e–001	1.33e–001	1.72e–001
M2-RBFN	0.94e–001	0.75e–001	0.52e–001	0.76e–001

Table 2 Comparison of the intrinsic torque (IT) obtained at CSIRO and the results predicted by M2-RBFN method for unsteamed wool worsted yarns around 30 days after spinning and measured in dry conditions

Unsteamed yarns in dry condition (30 days ± 3)			
Count (tex)	Twist (tpm)	IT using linearization	IT predicted by the present method
30	288	0.812	0.887
50	537	1.840	2.062
80	495	2.633	2.855

x_1 $h^1(x)$ w^1

x_i $h^j(x)$ w^j $f(\mathbf{x})$

w^m

x_d $h^m(x$

Fig. 1 Architecture of a fully connected RBFN $\mathbf{x} \in R^n; \{w^j\}_{j=1}^m$ is the set of weights of the NN.

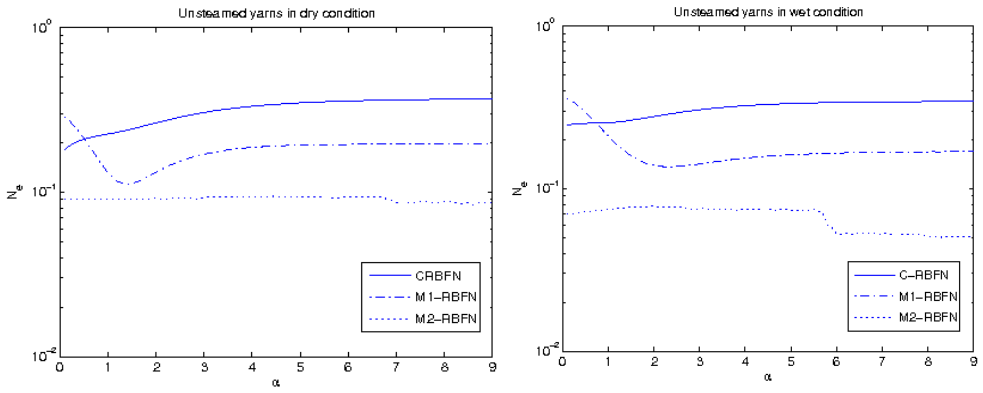

Figure 2 Modelling the torque function for un-steamed yarns: L2 norm error (N_e) with respect to coefficient α Solid line: the C-RBFN approach, dash-dot line: the M1-RBFN, dashed line: the M2-RBFN; the figure on the left is in dry conditions and on the right is in wet conditions.

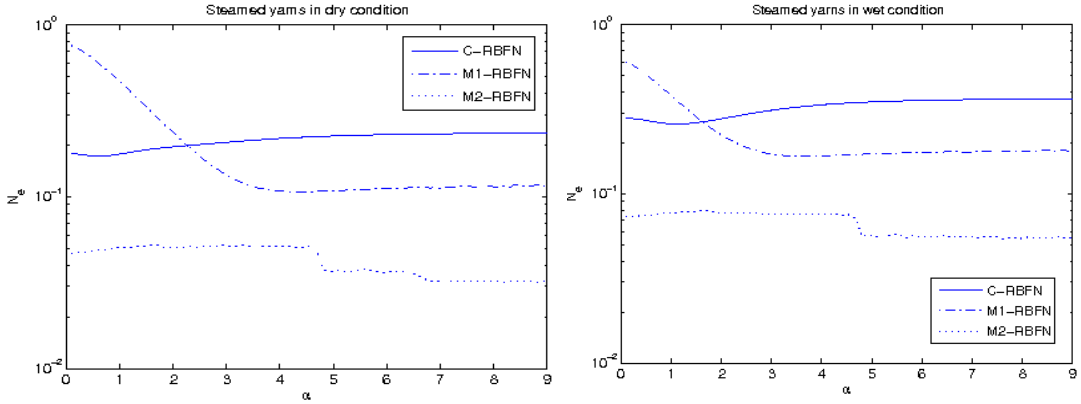

Figure 3 Modelling of torque function for steamed yarns: error norm (Ne) with respect to the coefficient α Solid line; the C-RBFN, dash-dot line: the M1-RBFN, dashed line: the M2-RBFN; the figure on the left is in dry conditions and on the right is in wet conditions.

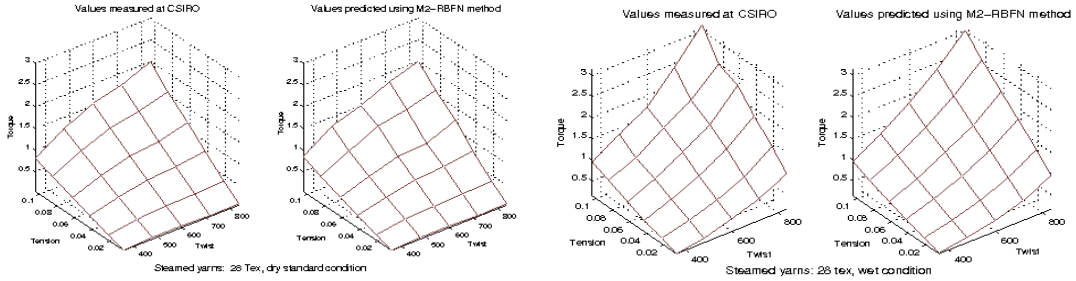

Figure 4 Predicted torque (μNm) with respect to twist (tpm) and applied tension (N) using the M2-RBFN method compared with experimental measurement at CSIRO for the 28 tex yarn; the left figure is for dry conditions (R^2 = 0.991) and right is for wet conditions (R^2 = 0.983).

.

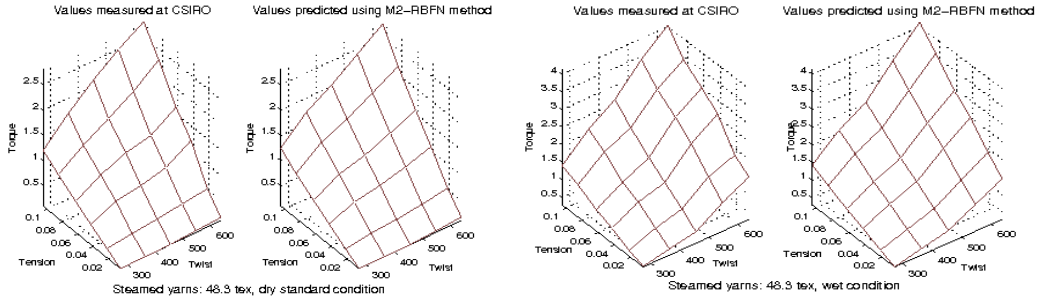

Figure 5 Torque (μNm) with respect to twist (tpm) and applied tension (N) for the 48.3 tex yarn using results of the experimental measurement at CSIRO and the M2-RBFN-based methods; the left figure is for dry conditions (R^2 = 0.985) and right is for wet conditions (R^2 = 0.988).

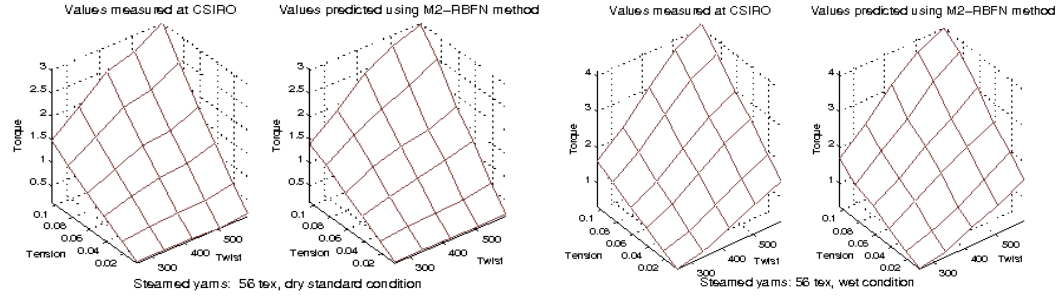

Figure 6 Torque (μNm) with respect to twist (tpm) and applied tension (N) for the 56 tex yarn, using results of the experimental measurements at CSIRO and theM2-RBFN-based methods; the left figure is for dry conditions (R^2 = 0.987) and right is for wet conditions (R^2 = 0.994).

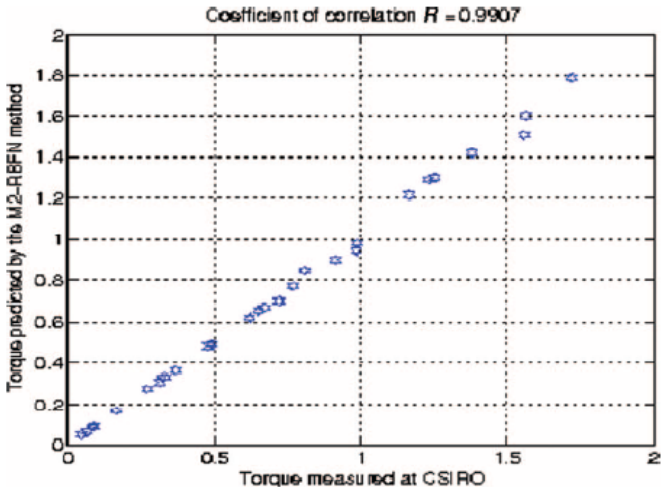

Figure 7 The plot of measured torque and predicted torque for the dry data shown in figure 4 ($R^2 = 0.991$).

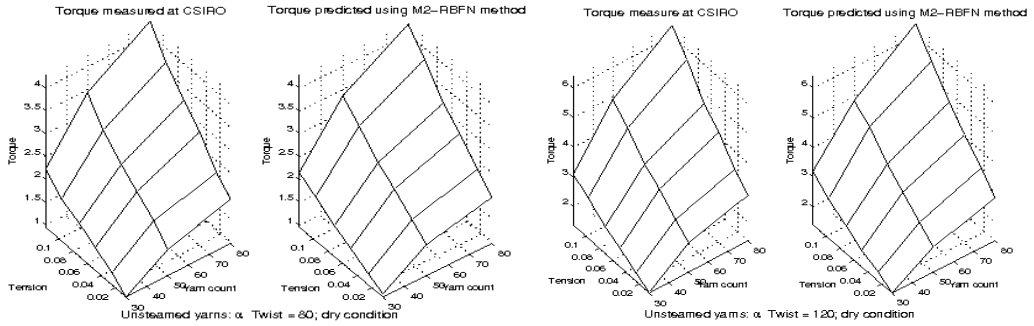

Figure 8 Torque (μNm) with predicted yarn count and applied tension (N) using results of the experimental measurement in dry conditions at CSIRO and the M2-RBFN-based methods; the left figure is for a metric twist factor of 80 ($R^2 = 0.970$) and right is for a metric twist factor of 120 ($R^2 = 0.978$).

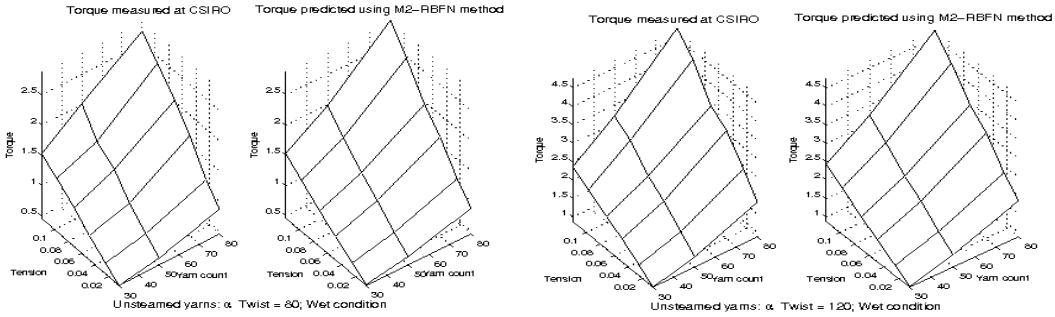

Figure 9 The torque (μNm) with respect to yarn count and applied tension (N) using results of the experimental measurement in wet conditions at CSIRO and the M2-RBFN-

based method: the left figure is for a metric twist factor of 80 (R^2 = 0.963) and right is for a metric twist factor of 120 (R^2 = 0.967).

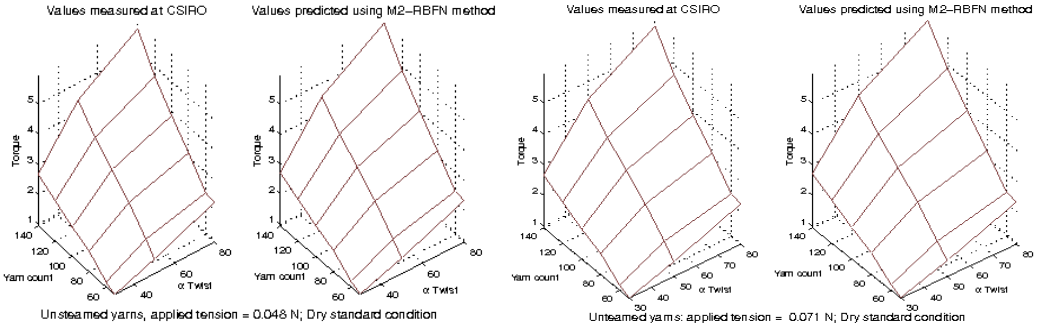

Figure 10 The torque (μNm) with respect to yarn count and metric twist factor using results of the experimental measurement in the dry conditions at CSIRO and the M2-RBFN-based method: The left figure is for applied tension = 0.048 N (R^2 = 0.971) and the right is for applied tension = 0.071 N (R^2 = 0.961).

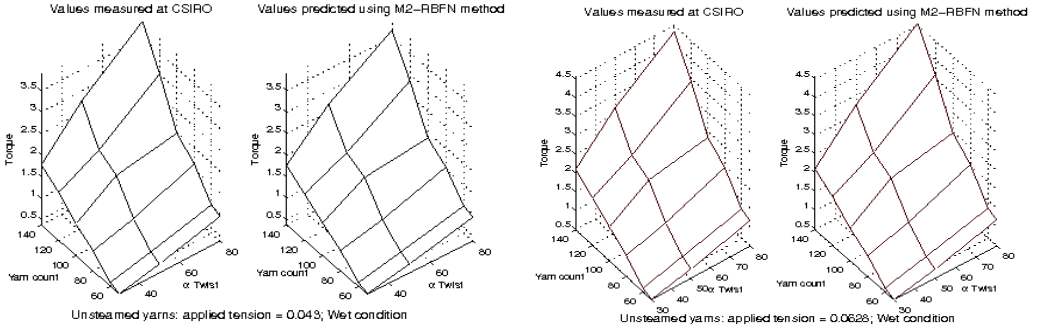

Figure 11 The torque with respect to yarn count, twist, and applied tension: the plots of torque versus yarn count and twist using results of the experimental measurement in the wet conditions at CSIRO and the M2-RBFN-based method: The left figure is for applied tension = 0.043 N (R^2 = 0.968) and the right is for applied tension = 0.0628 N (R^2 = 0.959).